Original Paper

Cells Tissues Organs

Cells Tissues Organs 2007;186:129–140
DOI: 10.1159/000103015

Accepted after revision: February 27, 2007
Published online: May 21, 2007

Macro- and Microstructure of the Superior Cervical Ganglion in Dogs, Cats and Horses during Maturation

Emerson Ticona Fioretto[a] Rogério Navarro de Abreu[c]
Marcelo Fernandes de Souza Castro[b] Wanderley Lima Guidi[a]
Antonio Augusto Coppi Maciel Ribeiro[a]

[a]Department of Surgery, College of Veterinary Medicine, University of São Paulo and [b]Institute of Health Sciences, Paulista University, São Paulo, [c]UNIFEOB (Fundação de Ensino Octávio Bastos), São João da Boa Vista, Brazil

Key Words
Superior cervical ganglion · Maturation · Post-natal development

Abstract
The superior cervical ganglion (SCG) provides sympathetic input to the head and neck, its relation with mandible, submandibular glands, eyes (second and third order control) and pineal gland being demonstrated in laboratory animals. In addition, the SCG's role in some neuropathies can be clearly seen in Horner's syndrome. In spite of several studies published involving rats and mice, there is little morphological descriptive and comparative data of SCG from large mammals. Thus, we investigated the SCG's macro- and microstructural organization in medium (dogs and cats) and large animals (horses) during a very specific period of the post-natal development, namely maturation (from young to adults). The SCG of dogs, cats and horses were spindle shaped and located deeply into the bifurcation of the common carotid artery, close to the distal vagus ganglion and more related to the internal carotid artery in dogs and horses, and to the occipital artery in cats. As to macromorphometrical data, that is ganglion length, there was a 23.6% increase from young to adult dogs, a 1.8% increase from young to adult cats and finally a 34% increase from young to adult horses. Histologically, the SCG's microstructure was quite similar between young and adult animals and among the 3 species. The SCG was divided into distinct compartments (ganglion units) by capsular septa of connective tissue. Inside each ganglion unit the most prominent cellular elements were ganglion neurons, glial cells and small intensely fluorescent cells, comprising the ganglion's morphological triad. Given this morphological arrangement, that is a summation of all ganglion units, SCG from dogs, cats and horses are better characterized as a ganglion complex rather than following the classical ganglion concept. During maturation (from young to adults) there was a 32.7% increase in the SCG's connective capsule in dogs, a 25.8% increase in cats and a 33.2% increase in horses. There was an age-related increase in the neuronal profile size in the SCG from young to adult animals,

Abbreviations used in this paper

SCG	superior cervical ganglion
SIF	small intensely fluorescent

KARGER

Fax +41 61 306 12 34
E-Mail karger@karger.ch
www.karger.com

1422–6405/07/1862–0129$23.50/0

Accessible online at:
www.karger.com/cto

Dr. Antonio Augusto Coppi Maciel Ribeiro
Faculdade de Medicina Veterinária e Zootecnia
Departamento de Cirurgia, Universidade de São Paulo (USP)
Av. Prof. Dr. Orlando Marques de Paiva, 87, São Paulo, CEP 05508-000 (Brazil)
Tel. +55 11 3091 1314, Fax +55 11 3091 7805, E-Mail guto@usp.br

that is a 1.6-fold, 1.9-fold and 1.6-fold increase in dogs, cats and horses, respectively. On the other hand, there was an age-related decrease in the nuclear profile size of SCG neurons from young to adult animals (0.9-fold, 0.7-fold and 0.8-fold in dogs, cats and horses, respectively). Ganglion connective capsule is composed of 2 or 3 layers of collagen fibres in juxtaposition and, as observed in light microscopy and independently of the animal's age, ganglion neurons were organised in ganglionic units containing the same morphological triad seen in light microscopy.

Introduction

The autonomic nervous system in rats and in other mammals consists of a vast array of nerves and ganglia connected to the central nervous system on one side and to the viscera on the other side. The sympathetic cervical chain lies dorsally to the vagus nerve and ventrally to transverse processes of vertebrae and prevertebral muscles. Two ganglia are present in the neck region, the superior cervical ganglion (SCG) or cranial cervical ganglion and the caudal cervical ganglion or stellate ganglion (which includes the uppermost thoracic sympathetic ganglia); a small intermediate (middle) cervical ganglion is sometimes found [Hedger and Webber, 1976; Baljet and Drukker, 1979; Gabella, 2004].

The SCG, which is a paravertebral ganglion, provides sympathetic input to the head and neck as well as to the mandible, submandibular glands, pineal and eyes (second and third order control) in laboratory animals [Luebke and Wright, 1992; Hubbard et al., 1999; Moller and Liu, 1999; Hayakawa et al., 2000; Ladizesky et al., 2000]. In rats, the SCG is an attractive model because it is easily located and is used as a model to investigate neurobiological disorders. Furthermore, the SCG has relatively straightforward pre-ganglionic inputs and well-characterized target organs [Purves and Lichtman, 1978; Luebke and Wright, 1992].

In addition, the presence of adrenergic nerves in bone is well documented and several recent studies have reported the effects of sympathetic denervation, namely SCG ganglionectomy, on skeletal tissues. A reduction in periosteal bone apposition at the end of the first week following sympathectomy in rats was clearly demonstrated by Sandhu et al. [1987]. Furthermore, the effects of unilateral SCG ganglionectomy on bone mineral content and density of the rat's mandible has been shown by Ladizesky et al. [2000], who reported that bone modelling and remodelling are highly regulated processes in the mammalian skeleton and that the disruption of the sympathetic control of modelling may lead to various bone diseases.

On the other hand, the SCG's role in some neuropathies is clearly seen in Horner's syndrome as described by Bell et al. [2001] in humans and by Boydell [1995] and Panciera et al. [2002] in dogs. Indeed, several studies have been published on the SCG of stroke-prone rats due to its role in the innervation of cerebral vessels during stroke [Cardinali et al., 1981; Sadoshima et al., 1981; Sadoshima and Heistad, 1982; Coutard et al., 2003].

Nevertheless, in large mammals little is known about the SCG, although in the last 20 years they have been studied frequently with the help of pharmacology, electrophysiology, immunohistochemistry and biochemical techniques mostly in rats, mice and guinea pigs, especially because their innervation territory includes intracranial organs such as cerebral vessels, pineal and eye [Miolan and Niel, 1996].

In mammals, ageing, which is part of the post-natal development, is associated with decrements in cellular and physiological functions and a major incidence of degenerative diseases. These alterations are the result of interaction amongst many factors and one may say that ageing is therefore a multifaceted phenomenon [Szweda et al, 2003]. In the nervous system, the changes most frequently related are neuron loss, atrophy and hypertrophy [Cabello et al., 2002]. However, these claims are controversial because there are regional differences between various components of the nervous system amongst animal species [Finch, 1993; Vega et al., 1993].

Additionally, some quantitative studies have been published estimating the total number of SCG neurons during ageing in rats [Santer, 1991] or allometrically related changes in SCG neuron number in mammals of very different body weights, such as rats, capybaras and horses [Ribeiro et al., 2004].

Hence, in the present study our first aim was to find out whether or not ageing, especially maturation, would affect the morphological organization of the sympathetic nervous system of non-laboratory animals by looking at SCG's size, microstructure and ganglion neuron size.

Our second aim was that the current collected data would shed light on future investigations involving the use of large animal models (who are allometrically closer to humans) to pursue ageing studies on the autonomic nervous system as well as to elucidate a possible modulatory role of SCG in the cerebral vasculature innervation in stroke-affected humans and non-human patients.

Thirdly, all these data may help researchers to understand and treat animal sympathetic disorders such as Horner's syndrome [Panciera et al., 2002] and other animal neuropathies such as stroke [Campbell et al., 2000; Shaibani et al., 2006; Palmer, 2007] and epilepsy [Kokaia et al., 1994] which are related to SCG, as details of their diagnosis and therapy are still unclear to most neuroscientists and neurologists of large mammals.

Materials and Methods

Animals

Dogs

In this investigation, a total of 20 left SCG from 20 mongrel male dogs were used. The animals came from the Veterinary Hospital, College of Veterinary Medicine, University of São Paulo, Brazil. According to the animal's age, the specimens were divided into 2 groups.

Group 1 consisted of young dogs (1 month old; body weight 3–4 kg). In this group, 10 ganglia were used, 4 for gross anatomy description and 6 for the microscopic study (3 for semi-thin light microscopy and 3 for scanning electron microscopy).

Group 2 comprised adult dogs (12–14 months old; body weight 7–15 kg). In this group, 10 ganglia were used, 4 for gross anatomy description and 6 for the microscopic study (3 for semi-thin light microscopy and 3 for scanning electron microscopy).

Cats

In this investigation, a total of 30 left SCG from 30 cross-breed male cats were used. The animals came from the Veterinary Hospital, College of Veterinary Medicine, University of São Paulo, Brazil. According to the animal's age, the specimens were divided into 2 groups.

Group 1 consisted of young cats (1–2 months old; body weight 1–3 kg). In this group, 15 ganglia were used, 5 for gross anatomy description and 10 for the microscopic study (5 for semi-thin light microscopy and 5 for scanning electron microscopy).

Group 2 comprised adult cats (10–12 months old; body weight 5–7 kg). In this group, 15 ganglia were used, 5 for gross anatomy description and 10 for the microscopic study (5 for semi-thin light microscopy and 5 for scanning electron microscopy).

Horses

In this study, 20 left SCG from 20 cross-breed male horses were used. The animals came from the Veterinary Hospital, College of Veterinary Medicine, Octávio Bastos Foundation, São João da Boa Vista, Brazil. According to the animal's age, the specimens were divided into 2 groups.

Group 1 contained young horses (1–7 months old; body weight 100–220 kg). In this group, 10 ganglia were used, 4 for gross anatomy description and 6 for the microscopic study (3 for semi-thin light microscopy and 3 for scanning electron microscopy).

Group 2 consisted of adult horses (12–24 months old; body weight 250–450 kg). In this group, 10 ganglia were used, 4 for gross anatomy description and 6 for the microscopic study (3 for semi-thin light microscopy and 3 for scanning electron microscopy).

Gross Anatomy Study

Dead animals (dogs, cats and horses) were injected with a red-stained (Suvinil S/A) latex bicentrifugate CIS I-4 polyisoprene via the thoracic aorta and perfused with a 20% formaldehyde solution in PBS (0.1 M, pH 7.4).

A ventral midline incision was made from the intermandibular space to the middle cervical region. The sternomastoid muscle was deflected to expose the left common carotid artery, internal jugular vein and vagosympathetic nerve trunk. By dissecting these structures, it was possible to observe the left SCG and branches of the common carotid artery. The sternomastoid, sternooccipital and digastric muscles, and the thyreoid gland were dissected for a full observation of SCG.

SCG and their nerve trunks were dissected in their entirety and immersed in a 60% acetic acid alcoholic solution and 20% hydrogen peroxide aqueous solution in order to permit a better identification of all nerve structures. Each ganglion was measured for its long and short axes using a digital pachymeter (Digimess®). The length or long axis was taken as the distance between the 2 poles and the width or short axis as the major transverse distance.

The microdissection was pursued using a M651 Leica® surgical microscope with 6×, 10×, 16× and 20× objective lenses.

Histology

Animals (cats, dogs and horses) were killed using acepromazine 0.2% (0.2–1.0 mg/kg, intravenously) and an overdose of anaesthetic (Na pentobarbitone, 80 mg/kg, intravenously) in connection with other experiments carried out by several research groups at the Veterinary Hospital, College of Veterinary Medicine, University of São Paulo, Brazil. With a skin incision along the neck, the left common carotid artery and the left jugular vein were exposed. A bulbed cannula was inserted into the common carotid artery and about 100 ml of pre-wash fluid (PBS, Na nitrite and heparin) was perfused, followed by about 200 ml of fixative (5% glutaraldehyde and 1% formaldehyde in 100 mM sodium cacodylate) used at room temperature. Drainage was obtained by slitting the jugular vein with the same procedure pursued by Gabella et al. [1988].

In all 3 species, the neurovascular bundle was isolated at the base of the neck. Vagus nerve and cervical sympathetic trunk were dissected from the common carotid artery. The left cervical sympathetic trunk was followed cranially along the common carotid artery, while removing surrounding muscles, up to the cranial cervical ganglion (SCG).

All nerve trunks issuing from the ganglion were cut and the ganglion was dissected in its entirety.

Semi-Thin Section Light Microscopy

The ganglia from cats, dogs and horses were placed in fresh fixative (the same fixative used for perfusion) for 1–2 weeks before embedding. The ganglia were cut transversely with a razor blade and a calibrated ruler into 3 or 5 slabs comprising the whole ganglion.

All the ganglion slabs were washed thoroughly in sodium cacodylate buffer, post-fixed in 2% osmium tetroxide in cacodylate buffer, block stained with a saturated solution of uranyl acetate, dehydrated in graded ethanols and propylene oxide, and embedded in resin (Araldite). The resin was cured at 70°C for 3 days.

Morphometry

Each ganglion slab was exhaustively cut and for the morphometric study 70–80 serial sections were cut at 2 μm thickness using a Leica Ultracut UCT ultramicrotome with glass knives. For each ganglion, 30 consecutive sections were collected on glass slides, stained with toluidine blue and mounted under a cover slip with a drop of Araldite. A test system comprised of 8 different unbiased counting frames was put over each section field's image projected on a computer screen. The total sampled area in the test systems was 40,000 μm^2.

A fraction of the counting frames was random uniform and systematically sampled, using a random start between 1 and fraction. The sampled field's images were observed on a computer screen using a Leica DMR microscope coupled with a Leica DFC 300FX digital camera. In each counting frame (with a surrounding guard area), only the neurons located inside the counting frame and not outside the forbidden lines were measured [Gundersen, 1977]. This approach was also adopted in a three-dimensional view 'brick counting frame' [Howard and Reed, 2005]. Each neuron received the same number in all serial sections, and its largest perikaryon profile as well as its largest nuclear profile were identified and therefore measured for the cross-sectional area using the Leica Q-Win image analysis system. In each animal, a total of 100 neurons and 70 neuronal nuclei were measured.

Scanning Electron Microscopy

The ganglia from dogs, cats and horses were cut transversely with a razor blade and a calibrated ruler into 3 or 5 slabs comprising the whole ganglion, digested chemically and prepared for scanning electron microscopic study in accordance with Fujiwara and Uehara [1980], Baluk and Fujiwara [1984], Matsuda and Uehara [1984], Baluk [1986], Baluk and Gabella [1987] and Chunhabundit et al. [1993]. Thus, all ganglion slabs were digested with trypsin I (Sigma; 2.5 mg/ml), in PBS at 37°C for 1 h, collagenase I (Sigma; 8 mg/ml) at 37°C for 20 h and collagenase III (Sigma; 1 mg/ml) at 37°C for 1 h. Later, fragments were immersed in a 37% HCl aqueous solution for 20 min at 60°C with constant agitation and fixed in 2.5% glutaraldehyde solution (Merck) and in PBS (pH 7.4, 0.1 M) for 24 h at room temperature.

All ganglion slabs were washed in PBS, post-fixed in 1% osmium tetroxide in PBS (0.1 M) for 2 h, dehydrated in graded ethanols, critical point dried in a CPD 020 (Balzers Union®), mounted on metal stubs and sputter coated with gold in an Emitech® K550. The material was finally examined and photographed under a 435VP Leo® scanning electron microscope.

Statistical Analysis

Quantitative results are shown as means with coefficients of variation given in parentheses (coefficient of variation = SD/mean). For continuous distribution data (ganglion measurements, cell area and nuclear area), the analysis accounted for the age effect between groups within each animal species (young and adult animals), using one-way ANOVA with the Statistical Analysis System software, version 8.02 (SAS). In case of significant data ($p < 0.05$), the t test was applied for multiple comparisons.

Results

Anatomy

In the 3 species studied, the SCG was located at the most cranial part of the cervical region, close to the base of the skull and represented the cranial portion of the sympathetic trunk which was associated with the vagus nerve forming the vagosympathetic trunk. The position of the SCG was close to the internal carotid artery in dogs and horses and to the occipital artery in cats (fig. 1).

In terms of topographic anatomy, the SCG is located dorsocranially to the larynx, craniomedially to the thyroid gland and ventrocaudally to the tympanic bulla in all species.

These ganglia are also related to the longus capitis muscle, to the hypoglossal nerve and they are very close to the distal vagus ganglion (fig. 1).

In all species studied, the SCG was white in colour and roughly spindle shaped, independent of the animal's age (fig. 1).

Nerve fibres of the sympathetic trunk join to the SCG in the caudal extremity by a single trunk. In addition, the number of connected fibres to the SCG in its cranial extremity varied and the internal carotid nerves (1–3 branches) and jugular nerves (1–2) were always seen. Two to 3 nerves were observed emerging from either the caudal or the ventral-lateral part of the ganglion and were directed to the external carotid artery. They were named external carotid nerves.

Macromorphometrical Data (Ganglion Size)

Dogs

In young dogs, ganglion length and width were 3.5 mm (0.05) and 1.8 mm (0.07), respectively. In adults, they were 4.4 mm (0.02) and 2.34 mm (0.11), respectively. Differences between groups were insignificant ($p = 0.3$).

Cats

In young cats, ganglion length and width were 3.3 mm (0.03) and 0.8 mm (0.17), respectively. In adults, they were 3.3 mm (0.02) and 1.6 mm (0.18), respectively. Differences between groups were insignificant ($p = 0.4$).

Horses

In young horses, ganglion length and width were 19.6 mm (0.01) and 5.9 mm (0.08), respectively. In adult horses, they were 26.3 mm (0.01) and 6.4 mm (0.03), respectively. Differences between groups were insignificant ($p = 0.4$).

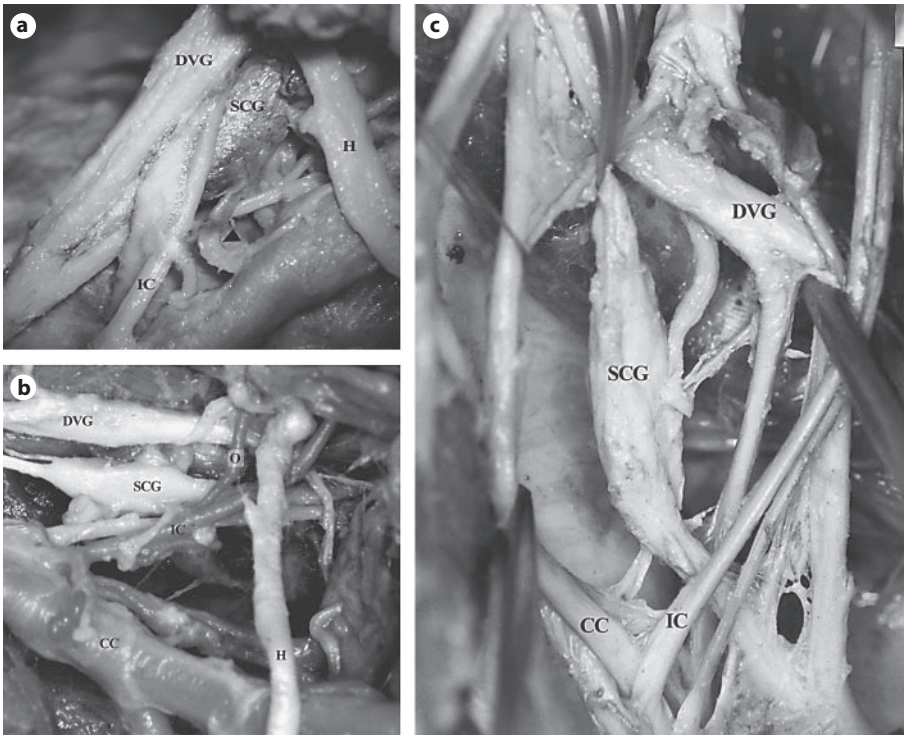

Fig. 1. Macrostructure of the SCG of an adult dog (**a**), cat (**b**) and horse (**c**). The SCG is located near the distal vagus ganglion (DVG) and related to internal carotid artery (IC), hypoglossal nerve (H), common carotid artery (CC) and occipital artery (O) in the cat.

Microstructure (Young and Adult Animals)

Under semi-thin section light microscopy, all ganglia were enveloped by a connective capsule which sent septa of connective tissue inside the SCG, dividing it into several ganglionic units. This general pattern was found in all 3 species either in young or adult animals.

The capsule of the ganglion was conspicuous and composed of layers of collagen fibres and flattened fibroblasts.

Therefore, each ganglion consisted of an agglomeration of clusters of neurons separated by nerve fibres, capillaries and prominent septa of collagen fibres (fig. 2).

In dogs the ganglion capsule thickness was 16.2 μm (0.22) in pups and 21.5 μm (0.26) in adults. No differences between age groups were observed ($p = 0.1$).

In cats the ganglion capsule thickness was 14.7 μm (0.24) in young animals and 18.5 μm (0.30) in adults. No differences between age groups were observed ($p = 0.13$).

In horses the ganglion capsule thickness was 51.4 μm (0.07) in young animals and 68.5 μm (0.08) in adults. No differences between age groups were observed ($p = 0.1$).

Each ganglionic unit was composed of various cell types and the units were separated from each other by nerve fibres, intraganglionic capillaries (placed encircling each ganglionic unit) and septa of collagen fibres (fig. 2). Given this cytoarchitectural arrangement, SCG was described as a true ganglionic complex rather than having a classical ganglion structure. Further, the capillaries were placed encircling each ganglionic unit (fig. 2). These intraganglionic capillaries were named inter-unit capillaries.

Within the ganglion, the stroma consisted of bundles of collagen fibres isolated or gathered into intraganglionic septa. The septa contained fibroblasts and blood vessels, mainly capillaries but also arterioles and venules.

Cell Types

The main cell types observed in the SCG were ganglion neurons, glial cells and small intensely fluorescent (SIF) cells which comprise the morphological ganglion triad. Ganglion neurons were generally spindle shaped and readily distinguishable due to their large size, clear nucleus and the evident nucleolus. Moreover, SIF cells were seen arranged in 2 different locations, namely close to neurons or encompassing tight clusters comprised of 2–5 cells in the proximity of blood vessels.

Ganglion neuron profiles were surrounded by 1–2 intraganglionic capillaries (in this case they were named intra-unit capillaries) as well as by 1–3 glial cell nuclei

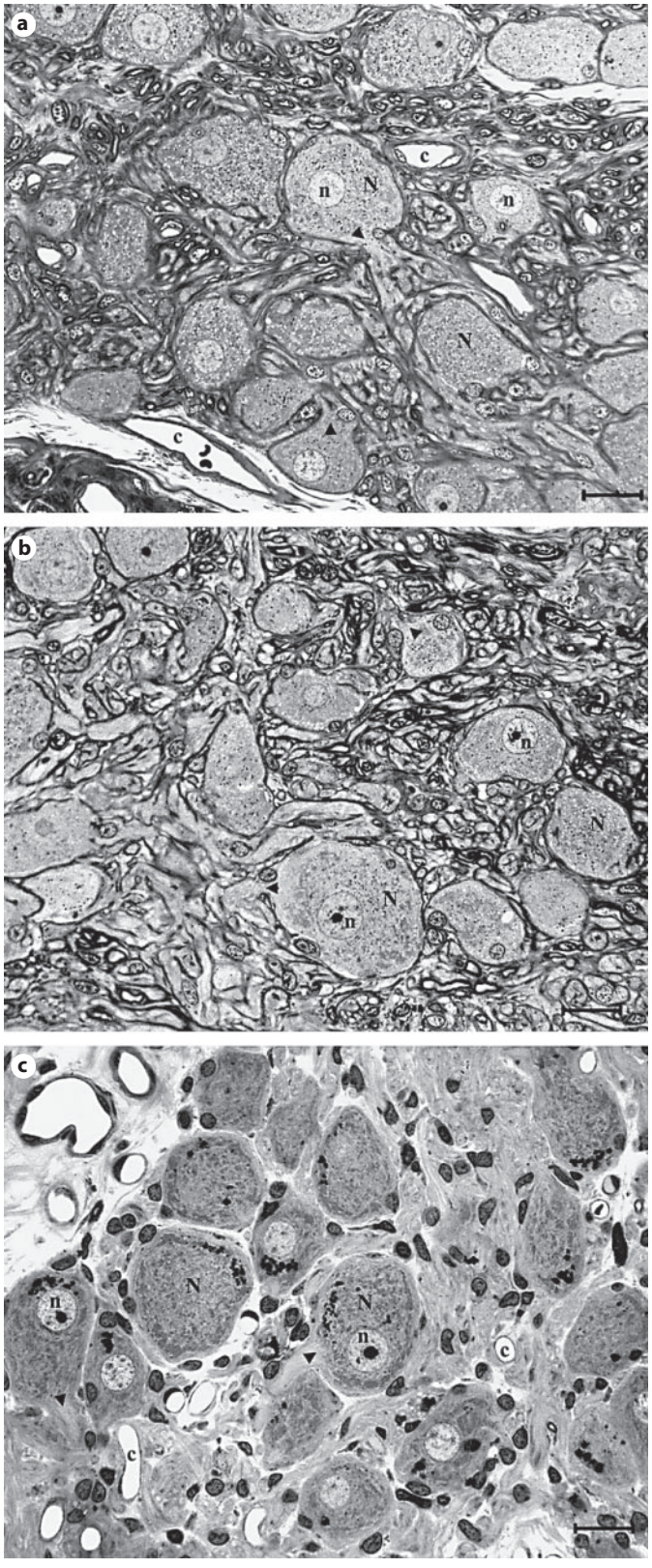

(satellite cells) and glial cell processes formed the ganglion neuron's glial capsule (fig. 3).

Furthermore, the ganglion neuron profiles were circular or more commonly spindle shaped in all species (fig. 2, 3).

In horses, the neuronal perikarya occupied a larger proportion of the sectional area than in dogs and cats and the neuropil was therefore proportionally less extensive (fig. 2).

All neurons were mononucleate and some nuclei were located in the centre of the perikaryon, while the majority were eccentric, but none resided at the periphery of the neuronal profile. Between 1 and 2 nucleoli were observed in each neuron nucleus.

Morphometry

Cell Profile Size

Dogs. The neuronal cross-sectional area was 475.3 μm^2 (0.17) in young dogs and 778.3 μm^2 (0.23) in adults. Differences between age groups were significant ($p = 0.02$).

Cats. The neuronal cross-sectional area was 357.1 μm^2 (0.22) in young cats and 678.5 μm^2 (0.21) in adults. Differences between age groups were significant ($p = 0.01$).

Horses. The neuronal cross-sectional area was 537.1 μm^2 (0.25) in young horses and 878.7 μm^2 (0.27) in adults. Differences between age groups were significant ($p = 0.03$).

Nuclear Profile Size

Dogs. The nuclear cross-sectional area was 70.3 μm^2 (0.19) in young dogs and 63.3 μm^2 (0.22) in adults. Differences between age groups were significant ($p = 0.04$).

Cats. The nuclear cross-sectional area was 67.1 μm^2 (0.21) in young horses and 47.5 μm^2 (0.25) in adults. Differences between age groups were significant ($p = 0.03$).

Fig. 2. Fine structure of the SCG of an adult dog (**a**), cat (**b**) and horse (**c**) in semi-thin sections photographed at the same magnification and showing several ganglion units. The horse's ganglion shows the largest neuropil, i.e. large spaces occupied by glial cells, nerve processes and inter-ganglionic unit capillaries (c). In the ganglion of dogs and even more in that of horses, the nerve cell bodies (N) are separated by post-ganglionic fibres (arrowheads), connective tissue and capillaries. Toluidine blue. Scale bar = 20 μm.

Horses. The nuclear cross-sectional area was 97.1 μm^2 (0.21) in young cats and 80.7 μm^2 (0.15) in adults. Differences between age groups were significant ($p = 0.03$).

Scanning Electron Microscopy

The surface aspects of SCG and its components were observed using scanning electron microscopy. The connective tissue of the ganglionic capsule covered all the ganglion and was composed of 2 or 3 layers of collagen fibres in juxtaposition and gave rise to intraganglionic connective tissue.

In order to describe the morphological aspects of the principal ganglion neurons, we digested the extracellular matrix and removed collagen fibres that covered ganglion neurons and other elements. Ganglion neurons had a spherical aspect, but more commonly elongated types (spindle shaped) were seen (fig. 4).

The ganglion neuron surface had a homogeneous aspect and presented branches of pre-ganglionic fibres that connected to ganglion neurons.

As observed in light microscopy and independently of the animal's age, ganglion neurons were organized in ganglionic units which were separated by collagen and nerve fibres. Moreover, satellite cells were observed in the vicinity of neurons. The satellite cell nuclei were spherical and located close to the other neuronal cells. The same cellular triad was observed using semi-thin sections under scanning electron microscopy.

Discussion

Anatomy

The SCG of dogs, cats and horses were located near the base of the skull and deep into the bifurcation of the common carotid artery, in the source of the external and internal carotid arteries close to the distal ganglion of

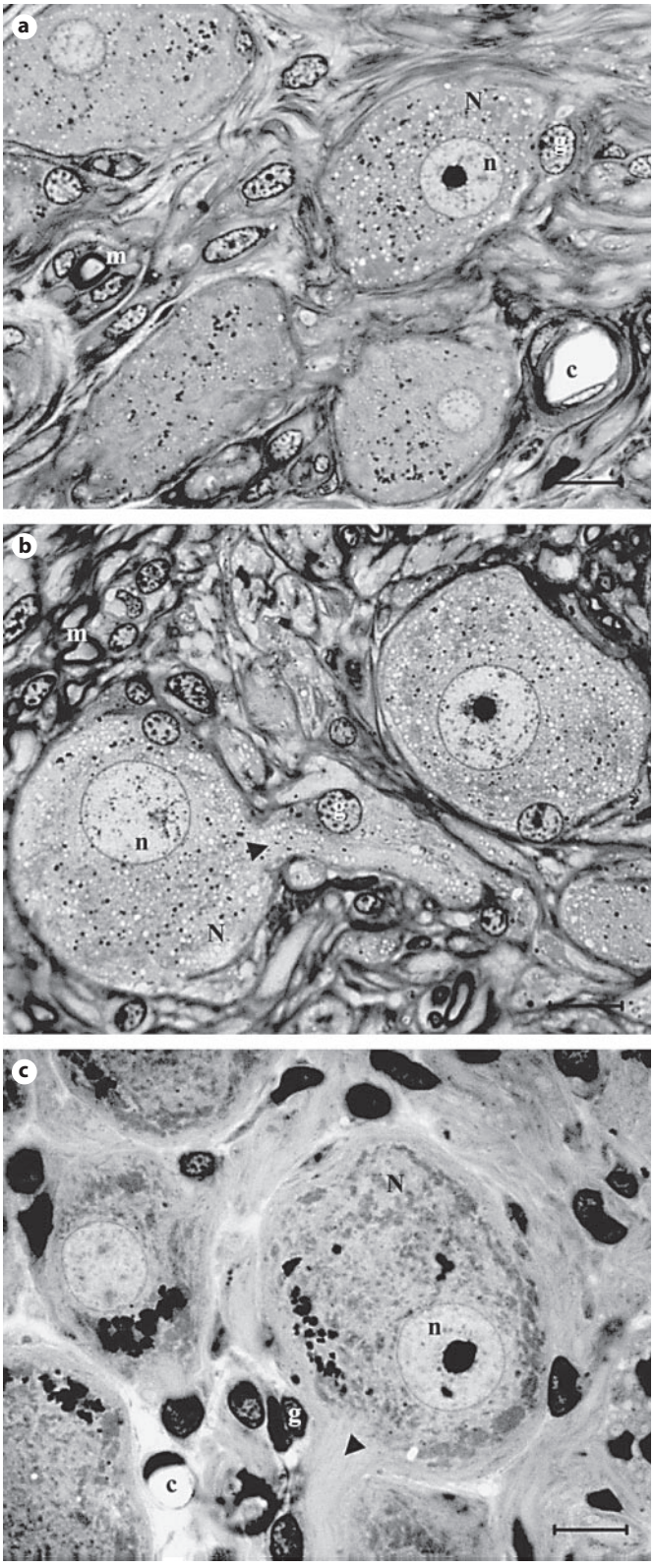

Fig. 3. High-magnification view of ganglia of an adult dog (**a**), cat (**b**) and horse (**c**) at the same magnification. Glial cell nuclei (g), myelinated axons (m), intra-ganglionic unit capillaries (c), neurons (N) and their nucleoli (n) and post-ganglionic fibres (arrowheads) can be recognised. Nuclei of glial cells (g) are visible in the large spaces between nerve cell bodies, especially in the horse. Toluidine blue. Scale bar = 10 μm.

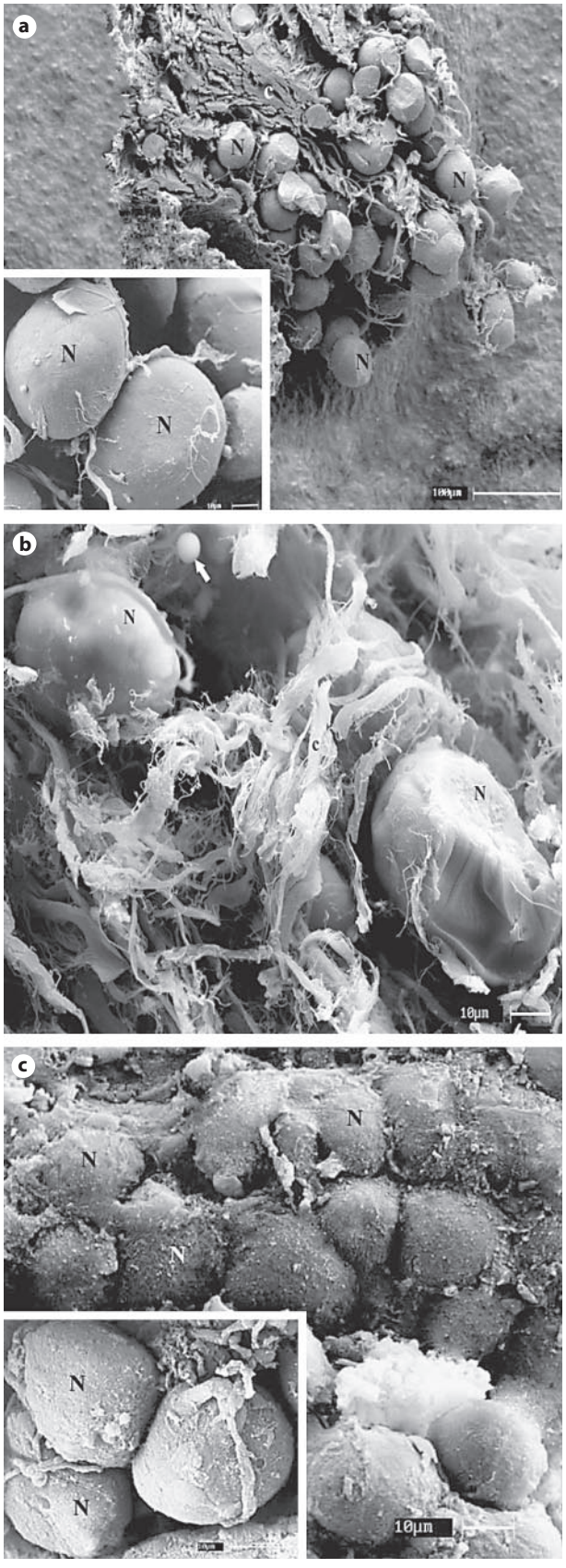

the vagus nerve and more related to the internal carotid artery in dogs and horses and to the occipital artery in cats. In the same way, sympathetic and parasympathetic nerve structures of young pigs (SCG and distal vagus ganglion) were just close to each other without any connection and located near the base of the skull and could descend to the first cervical vertebra level [Pospieszny and Bruzewicz, 1998; Kabak et al., 2005]. Hence, SCG was located deeply into the bifurcation of the common carotid artery and superficially related to the longus capitis muscle as in adult albino rats [Hedger and Webber, 1976].

Concerning the morphological aspects of the SCG in all species (young and adult animals), they were spindle shaped and white in colour. This morphological arrangement was independent of the animal's age and species. Further, a similar morphological feature was seen in adult rats [Hedger and Webber, 1976], though in pigs ganglion shape was very variable and complex, ranging from oval shaped to slightly resembling a triangle [Pospieszny and Bruzewicz, 1998; Kabak et al., 2005].

As to macromorphometrical data, that is ganglion length, there was a 23.6% increase from young to adult dogs, a 1.8% increase from young to adult cats and finally a 34% increase from young to adult horses. This finding is in agreement with the results reported by Ribeiro et al. [2004] (rats, capybaras and horses) and Gagliardo et al. [2005] (dogs) where the authors stated a positive correlation between body size and SCG size. The latter was expressed in those studies as the ganglion volume.

Reviewing the literature, several data concerning SCG's dimensions have been reported in different animal species, for example a length of 16.59–19.45 mm in young pigs [Kabak et al., 2005], 15–20 mm in camels [Cui et al., 1998], 3.1–3.4 mm in rats, 15.1–16.3 mm in adult capybaras and 17.1–24.8 mm in adult horses [Ribeiro et al., 2004], and 12.2–14.5 mm in young capybaras [Ribeiro, 2006].

From a surgical point of view, it may be useful to know macrostructural SCG dimensions as well as its accurate

Fig. 4. Scanning electron micrograph of SCG of an adult dog (**a**), cat (**b**) and horse (**c**) evidencing superficial details of ganglionic units which are constituted mainly by ganglion neurons (N) and glial cells (arrow). The ganglionic units are separated by intraganglionic septa of collagen fibres (c). Scale bars = 100 µm (**a**) and 10 µm (**b**, **c**).

localisation, especially when pursuing operative procedures in the neck of animals, for example in cervical tumours, Horner's syndrome [Boydell, 1995; Panciera et al., 2002], Wobbler syndrome [Nanai et al., 2006] or during the treatment of guttural pouch mycoses in horses [Freeman, 2006; Millar, 2006].

Microstructure

The SCG's microstructure was quite similar between young and adults and among the 3 species. Therefore, SCG was divided into distinct compartments by capsular septa of connective tissue as reported for mammalian sympathetic ganglia by Gabella et al. [1988], Szurszewski and King [1989], Szurszewski and Miller [1994], Miolan and Niel [1996], Schmidt [1996], Ribeiro et al. [2002], Gagliardo et al. [2003] and Ribeiro et al. [2004].

Gabella et al. [1988] described that the sheep's SCG is composed of several ganglion units, each one being constituted of neurons and glial capsule. In addition, we have found various cell types compounding the SCG, such as ganglion neurons, SIF cells, Schwann cells, fibroblasts, mast cells and capillaries limited by connective septa coming from the ganglion capsule and therefore forming several compartments or ganglionic units whose concept represents an expansion of that stated by Gabella et al. [1988] and also adopted by Ribeiro et al. [2002]. These authors have suggested that there are variations in the general architecture of the sympathetic ganglia in large mammals when compared to that in small laboratory rodents, such as rats [Ribeiro et al., 2004] and mice [Purves et al., 1986].

The fact is that in large mammals, SCG is, structurally, a ganglionic complex rather than a classical single paravertebral sympathetic ganglion such as in laboratory animals [Appenzeller, 1990; Szurszewski and Miller, 1994; Miolan and Niel, 1996; Ribeiro et al., 2002].

Inside each ganglionic unit the most prominent cellular elements were ganglion neurons, glial cells and SIF cells, which were altogether named as the ganglion morphological triad, similar to that reported for the dog's celiac and caudal mesenteric ganglia by Ribeiro et al. [2002] and Gagliardo et al. [2003], respectively. Given this morphological arrangement, the SCG from dogs, cats and horses is much better characterised as a ganglion complex, and this structural arrangement might be due to the presence of very specific SCG innervation territories and target organs as seen by injecting retrograde neurotracers that revealed the exact localisation of the labelled neurons in SCG [Bowers and Zigmond, 1979; Flett and Bell, 1991; Luebke and Wright, 1992; Andrews et al., 1996; Hayakawa et al., 2000].

As for SIF cells, Matthews and Raisman [1969] and Jew [1985] have reported the presence of small granule-containing cells which are distinct to sympathetic neurons and other satellite cells. These small granule-containing cells were identified as SIF cells and formed tight clusters associated with small capillaries and, as stated by Miolan and Niel [1996], may play a neuroendocrine role.

SIF cells were classified into 2 types: type 1 with granular vesicles ranging from 80 to 100 nm and type 2 with granular vesicles varying from 150 to 300 nm [Gabella, 2004]. This author also described that SIF cells presented synapses to pre-ganglionic fibres and few SIF cells had synaptic contacts to ganglion neurons. Furthermore, SIF cells which had afferent and efferent synapses were named interneurons.

With regards to the ganglion capsule thickness during the animal's maturation, there was a 32.7% increase in dogs (from young to adults), a 25.8% increase in cats (from young to adults) and a 33.2% increase in horses (from young to adults). In addition, comparatively, a 0.14-fold increase was observed from cats to dogs, a 2.2-fold increase from dogs to horses and finally a 2.6-fold increase from cats to horses.

In the literature, Ribeiro et al. [2004] have reported that the SCG capsule thickness in adults ranged from 15 to 30 μm in rats, from 30 to 70 μm in capybaras and from 60 to 80 μm in horses. More recently, for dog's inferior mesenteric ganglion capsule, Gagliardo et al. [2005] have reported ranges of 11.8–21.3 μm (pups), 17.6–21.3 μm (adults) and 16.7–28.3 (middle-aged animals). Ribeiro [2006] has reported a range of 30–50 μm for SCG from young capybaras which represents a 28.5% reduction in relation to adult capybaras. At present, it is not clear why ganglion capsule thickness increases in adults. Is this due to the presence of more connective tissue in adults which could be implicated in the protection of ganglion neurons? Or is it due to the requirement of increased blood supply (blood vessels in connective tissue) to the increased ganglion?

Morphometry

Within each animal species there was an age-related increase in the neuronal profile size in the SCG from young to adult animals, that is a 1.6-fold, 1.9-fold and 1.6-fold increase in dogs, cats and horses, respectively. On the other hand, there was an age-related decrease in the nuclear profile size of SCG neurons from young to adult

animals: 0.9-fold, 0.7-fold and 0.8-fold in dogs, cats and horses, respectively.

The increase in the neuronal profile size during post-natal development was also reported by Gagliardo et al. [2005] for the caudal mesenteric ganglion of dogs as well as for the SCG of capybaras during maturation [Ribeiro et al., 2004; Ribeiro, 2006].

The proportion of cell body occupied by the nuclei also changes during maturation. Generally speaking, the fraction of cell body occupied by the nucleus decreases during post-natal development [Ribeiro et al., 2004; Gagliardo et al., 2005; Ribeiro, 2006], whereas the cell body itself increases. The same pattern was also found in the present study, that is a 0.4- to 0.5-fold decrease in the nucleus-cell body ratio from young to adult dogs, cats and horses, as well as in rabbit spinal ganglion neurons with ageing [Ledda et al., 2000].

This ratio decreases when the area occupied by cytoplasm increases compared to the nuclear area and that seems to be the case during post-natal development [Ledda et al., 2000; Gagliardo et al., 2005].

As to the scanning electron microscopic study and as reported by Matsuda and Uehara [1984] and Chunhabundit et al. [1993], we observed a large amount of irregular connective tissue covering the surface of the ganglion neurons and it was therefore difficult to observe the morphological details of ganglion cells.

In order to solve this morphological question, longer digestion periods (20 h in collagenase I) were performed to expose the ganglion neuron surfaces as recommended by Baluk and Fujiwara [1984] and Matsuda and Uehara [1984].

Inside ganglionic units, neuron clusters were separated by septa of connective tissue confirming the same pattern which had been observed in light microscopy. Furthermore, neurons were spherical or spindle shaped which is in line with either circular or oval profiles observed in light microscopy and with the results reported by Matsuda and Uehara [1984] for the rat's dorsal root ganglia, where neurons were described as spindle shaped in bipolar neuroblasts, spherical in pseudo-unipolar neurons and possessing several short finger-like processes in multipolar cells.

There is little data in the literature concerning scanning electron microscopic studies on sympathetic ganglia. Barton and Causey [1958] and Chunhabundit et al. [1993] observed oval or polygonal neurons in the vicinity of the capillaries of common tree shrew's SCG and rat's SCG, respectively. In a further study published by Baluk and Fujiwara [1984], frog heart neurons were described as generally smooth with short stubbly projections which represent satellite cells attachment points.

Baluk [1986] has reported that on the surface of some ganglia there were tightly packed clusters of cells which were smaller than the smallest neurons, and that these probably correspond to clusters of small granular cells (or SIF cells). In the present paper, similar clusters were neither seen in dogs and cats nor in horses.

Various authors have studied both pre- and post-ganglionic processes in SCG by several methods [Kondo et al., 1980; Kiraly et al., 1989; Abdel-Magied, 1995]. In the present study, thick processes were seen associated with the cell body of ganglion neurons as well as thin intensely ramified processes. A meshwork of nerve fibres on the neurons' surface was also observed by Chunhabundit et al. [1993].

Remarks for Future Studies

In conclusion, this paper sheds light on some aspects of domestic carnivorous and equine SCG's post-natal development which was represented here by the period from young to adult animals (maturation period). The main aspects seen here were the macrostructure (gross anatomy) and microstructure (especially the ganglion organization in units and the morphological cellular triad, i.e. ganglion neurons, SIF cells and glial cells).

In addition, due to the fact that only 2 life stages were looked at, namely young and adult animals (maturation period), future studies should concentrate on more age groups per animal species (foetus, newborn and middle-aged animals) and apply stereological methods in order to figure out possible changes in the total number of neurons during ageing (in both pre- and post-natal development periods) as well as to elucidate the mechanisms of a possible neurogenesis (using mitosis markers: BrdU, activin, Ki-67) or cell death (through apoptosis markers: caspases), the details of which are still unclear.

In addition, the use of retrograde neurotracers as well as DiI injections would clarify whether or not there is any relation between the ganglionic units of a compartmented SCG in large mammals and its innervation territories and target organs, i.e. whether SCG morphological units are true functional units in large animals.

By taking into account all of this, and seeing this study from a functional and applied point of view, it is expected that the current data may throw light on forthcoming investigations involving the use of large animal models (that are allometrically closer to humans) to pursue ageing studies on the autonomic nervous system as well as to

elucidate a possible SCG modulatory role in the cerebral vasculature innervation in stroke-affected humans and non-human patients. Furthermore, all these data may support the understanding and treatment of animal neuropathies such as Horner's syndrome, stroke and epilepsy, whose diagnosis and therapy are still unclear to most veterinary neurologists.

Acknowledgement

The authors thank FAPESP (Fundação de Amparo à Pesquisa do Estado de São Paulo; application No. 00/06417-0) for financial support.

References

Abdel-Magied, E.M. (1995) Fine structure of nerve endings and junctions in the superior cervical ganglion of the camel *(Camelus dromedarius)*. Anat Histol Embryol *24:* 117–121.

Andrews, T.J., C. Thrasivoulou, W. Nesbit, T. Cowen (1996) Target-specific differences in the dendritic morphology and neuropeptide content of neurons in the rat SCG during development and aging. J Comp Neurol *368:* 33–44.

Appenzeller, O (1990) Anatomy and histology; in Appenzeller, O (ed): The Autonomic Nervous System. Oxford, Elsevier, pp 1–10.

Baljet, B., J. Drukker (1979) The extrinsic innervation of the abdominal organs in the female rat. Acta Anat (Basel) *104:* 243–267.

Baluk, P (1986) Scanning electron microscopic studies of bullfrog sympathetic neurons exposed by enzymatic removal of connective tissue elements and satellite cells. J Neurocytol *15:* 85–95.

Baluk, P., T. Fujiwara (1984) Direct visualization by scanning electron microscopy of the preganglionic innervation and synapses on the true surfaces of neurons in the frog heart. Neurosci Lett *51:* 265–270.

Baluk, P., G. Gabella (1987) Scanning electron microscopy of the muscle coat of the guinea-pig small intestine. Cell Tissue Res *250:* 551–561.

Barton, A.A., G. Causey (1958) Electron microscopic study of the superior cervical ganglion. J Anat *92:* 339–407.

Bell, R.L., N. Atweh, M. Ivy, P. Possenti (2001) Traumatic and iatrogenic Horner syndrome: case reports and review of the literature. J Trauma *51:* 400–404.

Boydell, P (1995) Idiopathic Horner's syndrome in the golden retriever. J Small Anim Pract *36:* 382–384.

Bowers, C.W., R.E. Zigmond (1979) Localization of neurons in the rat superior cervical ganglion that project into different postganglionic trunks. J Comp Neurol *185:* 381–392.

Bowers, C.W., L.M. Dahm, R.E. Zigmond (1984) The number and distribution of sympathetic neurons that innervate the rat pineal gland. Neuroscience *13:* 87–96.

Cabello, C.R., J.J. Thune, H. Pakkenberg, B. Pakkenberg (2002) Ageing of substantia nigra in humans: cell loss may be compensated by hypertrophy. Neuropathol Appl Neurobiol *28:* 283–291.

Campbell, C.A., F.C. Barone, C.D. Benham, S.J. Hadingham, M.H. Harries, J.D. Harling, J.M. Hills, V.A. Lewis, K.B. Mackay, B.S. Orlek, R.F. White, A.A. Parsons, A.J. Hunter (2000) Characterisation of SB-221420A – a neuronal Ca^{2+} and Na^{+} channel antagonist in experimental models of stroke. Eur J Pharmacol *401:* 419–428.

Cardinali, D.P., M.I. Vacas, P.V. Gejman (1981) The sympathetic superior cervical ganglia as peripheral neuroendocrine centers. J Neural Transm *52:* 1–21.

Chunhabundit, P., S. Thongpila, C. Cherdchu, R. Somana (1993) Cytoarchitecture of the common tree shrew *(Tupaia glis)* superior cervical ganglion. Acta Anat (Basel) *148:* 213–218.

Coutard, M., P. Mertes, P. Mairose, M. Osborne-Pellegrin, J.B. Michel (2003) Arterial sympathetic innervation and cerebrovascular diseases in original rat models. Auton Neurosci *104:* 137–145.

Cui, S., J.L. Wang, Z.M. Xie (1998) The gross anatomy of the cranial cervical ganglion and its branches in the Bactrian camel *(Camelus bactrianus)*. Vet Res Commun *22:* 1–5.

Finch, C.E. (1993) Neuron atrophy during aging: programmed or sporadic? Trends Neurosci *6:* 104–110.

Flett, D.L., C. Bell (1991) Topography of functional subpopulations of neurons in the superior cervical ganglion of the rat. J Anat *177:* 55–66.

Freeman, D.E. (2006) Long-term follow-up on a large number of horses that underwent transarterial coil embolisation (TCE) for guttural pouch mycosis (GPM). Equine Vet J *38:* 271.

Fujiwara, T., Y. Uehara (1980) Scanning electron microscopy of myenteric plexus: a preliminary communication. J Electron Microsc *29:* 397–400.

Gabella, G., P. Trigg, H. McPhail (1988) Quantitative cytology of ganglion neurons and satellite glial cells in the superior cervical ganglion of the sheep: relationship with ganglion neuron size. J Neurocytol *17:* 753–769.

Gabella, G. (2004) The Rat Autonomic Nervous System. London, Academic Press.

Gagliardo, K.M., W.L. Guidi, R.A. da Silva, A.A.C.M. Ribeiro (2003) Macro and microstructural organization of the dog's caudal mesenteric ganglion complex (*Canis familiaris*-Linnaeus, 1758). Anat Histol Embryol *32:* 236–243.

Gagliardo, K.M., J.C.C. Balieiro, R.R. de Souza, A.A.C.M. Ribeiro (2005) Postnatal-related changes in the size and total number of neurons in the caudal mesenteric ganglion of dogs: total number of neurons can be predicted from body weight and ganglion volume. Anat Rec A Discov Mol Cell Evol Biol *286:* 917–929.

Gundersen, H.J.G. (1977) Notes on the estimation of the numerical density of arbitrary profiles: the edge effect. J Microsc *111:* 219–223.

Hayakawa, T., M. Itoh, T. Miki, T. Kaneto, H. Tomiyama, Y. Takeuchi (2000) Sympathetic fibres innervating the extraocular muscles: cells of origin in the cat superior cervical ganglion. Okajimas Folia Anat Jpn *77:* 119–124.

Hedger, J.H., R.H. Webber (1976) Anatomical study of the cervical sympathetic trunk and ganglia in the albino rat *(Mus norvegicus albinos)*. Act Anat *96:* 206–217.

Howard, C.V., M.G. Reed (2005) Unbiased Stereology: Three-Dimensional measurement in Microscopy. London, BIOS Scientific Publishers.

Hubbard, W.C., J.C. Robinson, K. Schmidt, J.W. Rohen, E.R. Tamm, P.L. Kaufman (1999) Superior cervical ganglionectomy in monkeys: effects on refraction and intraocular pressure. Exp Eye Res *68:* 637–639.

Jew, J.Y. (1985) Histofluorescence and ultrastructural observations of small intensely fluorescent (SIF) cells in the superior sympathetic ganglion of the guinea pig. Cell Tissue Res *241:* 529–538.

Kabak, M., I.O. Orhan, R.M. Haziroglu (2005) Macro anatomical investigations of the cranial cervical ganglion in domestic pig *(Sus scrofa domesticus)*. Anat Histol Embryol *34:* 199–202.

Kiraly, M., P. Favrod, M.R. Matthews (1989) Neuroneuronal interconnections in the rat superior cervical ganglion; possible anatomical bases for modulatory interactions revealed by intracellular horseradish peroxidase labelling. Neuroscience *33:* 617–642.

Kokaia, M., M.A. Cenci, E. Elmer, O.G. Nilsson, Z. Kokaia, J. Bengzon, A. Bjorklund, O. Lindvall (1994) Seizure development and noradrenaline release in kindling epilepsy after noradrenergic reinnervation of the subcortically deafferented hippocampus by superior cervical ganglion or fetal locus coerulus grafts. Exp Neurol *130:* 351–361.

Kondo, H., N.J. Dun, G.D. Pappas (1980) A light and electron microscopic study of the rat superior cervical ganglion cells by intracellular HRP-labeling. Brain Res *197:* 193–199.

Ladizesky, M., R. Cutrera, V. Boggio, C.E. Mautalen, D. Cardinali (2000) Effect of unilateral superior cervical ganglionectomy on bone mineral content and density of rat's mandible. J Auton Nerv Syst *78:* 113–116.

Ledda, M., L. Barni, L. Altieri, E. Pannese (2000) Decrease in the nucleo-cytoplasmic volume ratio of spinal ganglion neurons with age. Neurosci Lett *286:* 171–174.

Luebke, J.I., L.L. Wright (1992) Characterization of superior cervical ganglion neurons that project to the submandibular glands, the eyes, and the pineal gland in rats. Brain Res *589:* 1–14.

Matthews, M.R., G. Raisman (1969) The ultrastructure and somatic efferent synapses of small granule-containing cells in the superior cervical ganglion. J Anat *105:* 255–282.

Matsuda, S., Y. Uehara (1984) Prenatal development of the rat dorsal root ganglia: a scanning electron-microscopic study. Cell Tissue Res *235:* 13–18.

Millar, H. (2006) Guttural pouch mycosis in a 6-month-old filly. Can Vet J *47:* 259–261.

Miolan, J., J. Niel (1996) The mammalian sympathetic prevertebral ganglia: integrative properties and role in the nervous control of digestive tract motility. J Auton Nerv Syst *58:* 125–138.

Moller, M., W. Liu (1999) Innervation of the rat pineal gland by nerve fibres originating in the sphenopalatine, otic and trigeminal ganglia: a retrograde in vivo neuronal tracing study. Reprod Nutr Dev *39:* 345–353.

Nanai, B., R. Lyman, P. Bichsel (2006) Intraoperative use of ultrasonography during continuous dorsal laminectomy in two dogs with caudal cervical vertebral instability and malformation ('Wobblersyndrome'). Vet Surg *35:* 465–469.

Palmer, A.C. (2007) Pontine infarction in a dog with unilateral involvement of the trigeminal motor nucleus and pyramidal tract. J Small Anim Pract *48:* 49–52.

Panciera, R.J., J.W. Ritchey, J.E. Baker, M. DiGregorio (2002) Trigeminal and polyradiculoneuritis in a dog presenting with masticatory muscle atrophy and Horner's syndrome. Vet Pathol *39:* 146–149.

Pospieszny, N., S. Bruzewicz (1998) Morphology and development of the cervical part of the sympathetic trunk (pars cervicalis trunci sympathici) in the pig (*Sus scrofa* L.*)* during the prenatal period. Ann Anat *180:* 353–359.

Purves, D., J.W. Lichtman (1978) Formation and maintenance of synaptic connections in autonomic ganglia. Physiol Rev *58:* 821–862.

Purves, D., E. Rubin, W.D. Snider, J. Lichtman (1986) Relation of animal size to convergence, divergence and neuronal number in peripheral sympathetic pathways. J Neurosci *6:* 158–163.

Ribeiro, A.A.C.M. (2006) Size and number of binucleate and mononucleate superior cervical ganglion neurons in young capybaras. Anat Embryol *211:* 607–617.

Ribeiro, A.A.C.M., C.F. Elias, E.A. Liberti, W.L. Guidi, R.R. de Souza (2002) Structure and ultrastructure of the celiac-mesenteric ganglion complex in the domestic dog *(Canis familiaris)*. Anat Histol Embryol *31:* 344–349.

Ribeiro, A.A.C.M., C. Davis, G. Gabella (2004) Estimate of size and total number of neurons in superior cervical ganglion of rat, capybara and horse. Anat Embryol *208:* 367–380.

Sadoshima, S., D. Busija, M. Brody , D. Heistad (1981) Sympathetic nerves protect against stroke in stroke-prone hypertensive rats: a preliminary report. Hypertension *3:* 124–127.

Sadoshima, S., D. Heistad (1982) Sympathetic nerves protect the blood-brain barrier in stroke-prone spontaneously hypertensive rats. Hypertension *4:* 904–907.

Sandhu, H.S., M.S. Herskovits, I.J. Singh (1987) Effect of surgical sympathectomy on bone remodeling at rat incisor and molar root sockets. Anat Rec *219:* 32–38.

Santer, R.M. (2001) Sympathetic neuron numbers in ganglia of young and aged rats. J Auton Nerv Syst *33:* 221–222.

Schmidt, R.E. (1996) Neuropathology of human sympathetic autonomic ganglia. Micros Res Tech *35:* 107–121.

Shaibani, A., S. Khawar, W. Shin, T.A. Cashen, B. Schirf, M. Rohany, S. Kakodkar, T.J. Carroll (2006) First results in an MR imaging-compatible canine model of acute stroke. AJNR Am J Neuroradiol *27:* 1788–1793.

Szurszewski, J.H., B.F. King (1989) Physiology of prevertebral ganglia in mammals with special reference to inferior mesenteric ganglion; in S.G. Schultz, J.D. Wood, B.B. Rauner (eds): Handbook of Gastrointestinal Physiology. Bethesda, American Physiological Society, pp 519–577.

Szurszewski, J.H., S.M. Miller (1994) Physiology of the prevertebral ganglia; in L.R. Johnson (ed): Physiology of the Gastrointestinal Tract. New York, Raven Press, pp 795–878.

Szweda, P.A., M. Camouse, K.C. Lundberg, T.D. Oberley, L.I. Szweda (2003) Aging, lipofuscin formation, and free radical-mediated inhibition of cellular proteolytic systems. Ageing Res Rev *2:* 383–405.

Vega, J.A., B. Calzada, M.E. Del Valle (1993) Age-related changes in the mammalian autonomic and sensory ganglia; in F. Amenta (ed): Aging of the Autonomic Nervous System. London, CRC Press, pp 31–61.